



**POLITECNICO
DI TORINO**



Application of Smart Structures in Vibration Control and Energy Harvesting Technology

Department of Mechanical and Aerospace Engineering (DIMEAS), 2nd-Year Presentation of PhD, 25 September 2020

PhD Candidate: Mahmoud Askari

PhD Student of Mechanical Engineering

Email: mahmoud.askari@polito.it

Tutor: Prof. Cristiana Delprete

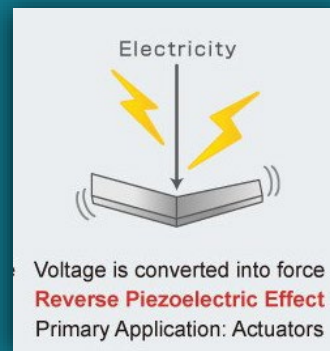
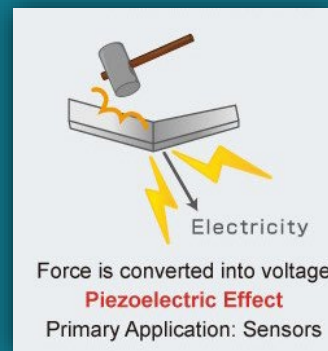
Full Professor of Mechanical Engineering

Email: cristiana.delprete@polito.it

Tutor: Prof. Eugenio Brusa

Full Professor of Mechanical Engineering

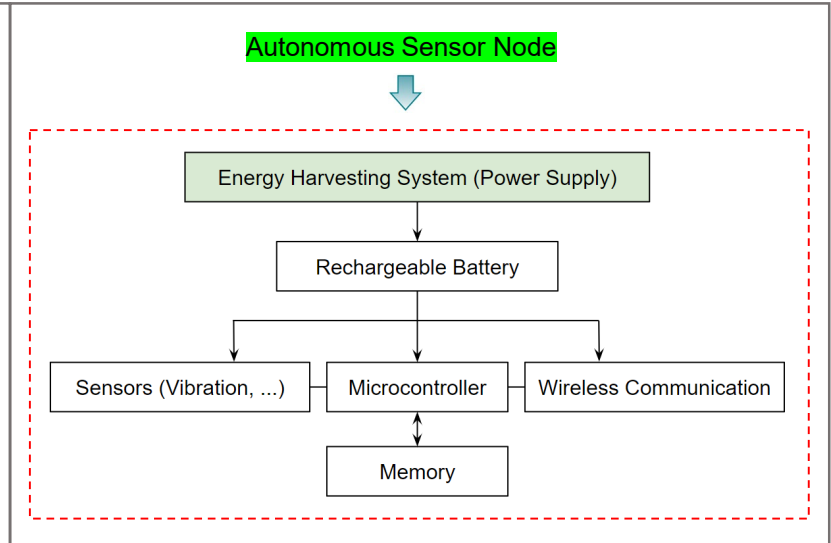
Email: eugenio.brusa@polito.it



- I.** To propose and design **energy harvesting systems** by using piezoelectric materials that have the capability of converting ambient vibration available in industrial machines into useful electric power.



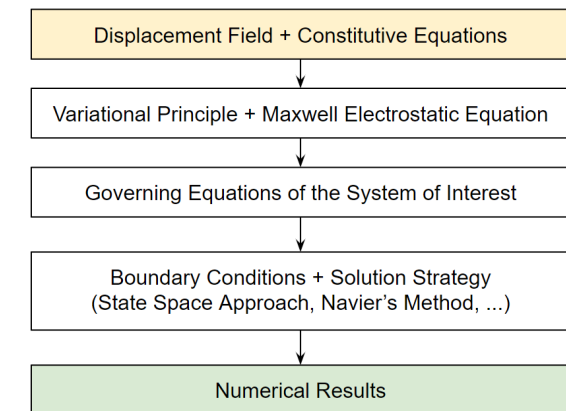
In this sense, the design of an autonomous condition monitoring sensor node is of interest. The final design will contain an accelerometer, a temperature sensor (in some cases), a wireless communication system, and an energy harvesting system for powering the entire device. The proposed device can operate autonomously and monitor the operating condition of the industrial machines such as rotors and rolling mills, to predict residual life and plan the maintenance activity in service, and to reduce the machine stop.



- II.** To provide a set of **analytical works** for electromechanical modeling of smart structures made of piezoelectric and graded materials containing porosity.



Employing the state space approach, the Navier's method, Galerkin approach and some other techniques, a set of analytical works have been done to analytically study the problems of free vibration, wave propagation, energy harvesting and buckling of smart structures such as beams, plates and shells having bimorph/unimorph configuration.



Design Of Autonomous Sensor Nodes

- ❖ A sensor node is a device generally consists of several sensors, a communication system and a power management system, basically used for condition monitoring. Available nodes on markets use batteries as their power source, thus having limited lifetime. In some cases, such nodes are not useable due to the harsh working condition of industrial machinery. To overcome these issues, energy harvesters are found to be a promising solution.

Components of the sensing system:

- ❑ A **three-axes accelerometer** has been provisionally selected on markets (Analog Devices ADXL346, three axes, range ± 16 g, 3.6 mW).
- ❑ A **temperature sensor** has been provisionally selected on markets (Microchip MCP9803, range -55/+125 C, 0.54 mW).
- ❑ A **wireless communication device** has been provisionally selected on markets (Texas Instruments CC2430, 250 kbit/s, 2.4 GHz, 60.48 mW in Tr. M.).
- ❑ The design of the **vibration piezoelectric energy harvesting system** is in progress.
- ❑ All the components will be included in a housing case, like in Fig. 1.
- ❑ The whole device can finally be bolted/bounded to the stationary part of the working machines for condition monitoring.

A set of FEM analyses including:

- **Modal analyses** have been done to see the resonance and mode shapes of the PEH.
- **Charge analysis** has been performed to see the generated voltage and power.
- **Stress/strain analyses** are in progress to see maximum displacement and stress within the PEH structure.
- The PEH layout will finally be optimized to generate the maximum power.



Fig. 1: Housing case

- ❖ A set of disc-like configurations made of piezoelectric bimorph/unimorph cantilevers have been proposed for vibration energy harvesting. This system will replace/recharge the batteries for prolonging the lifespan of the sensor nodes used in industry. Such energy harvesting systems can harvest the vibration available in working machinery, thus generating electric power, to be used for the operation of the whole sensing device.

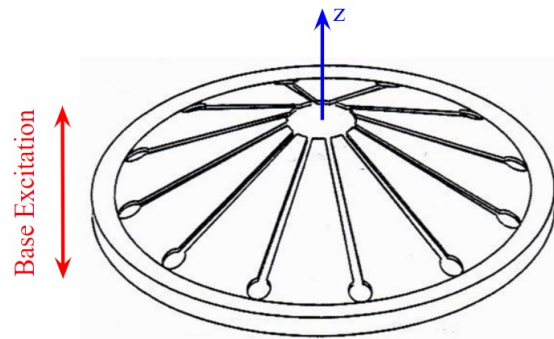


Fig. 1: A prediction of the final design

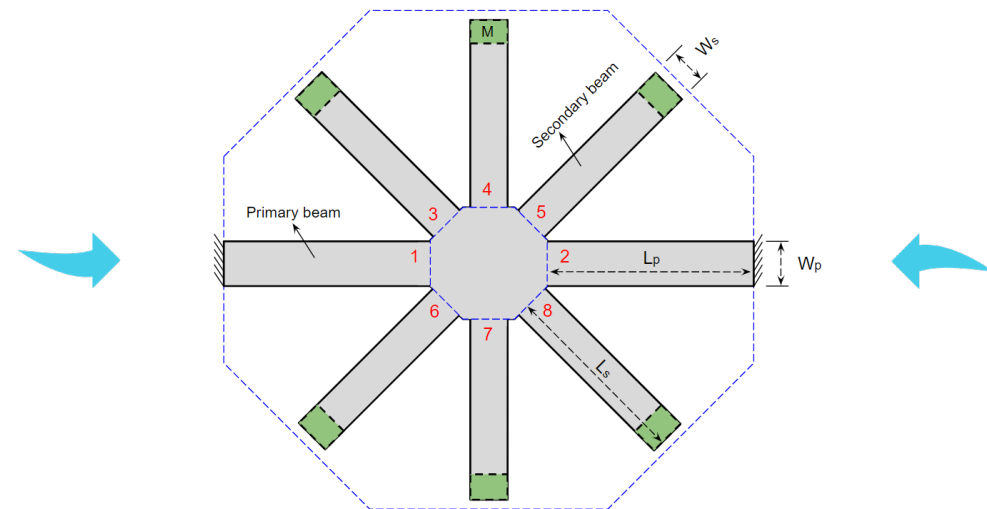
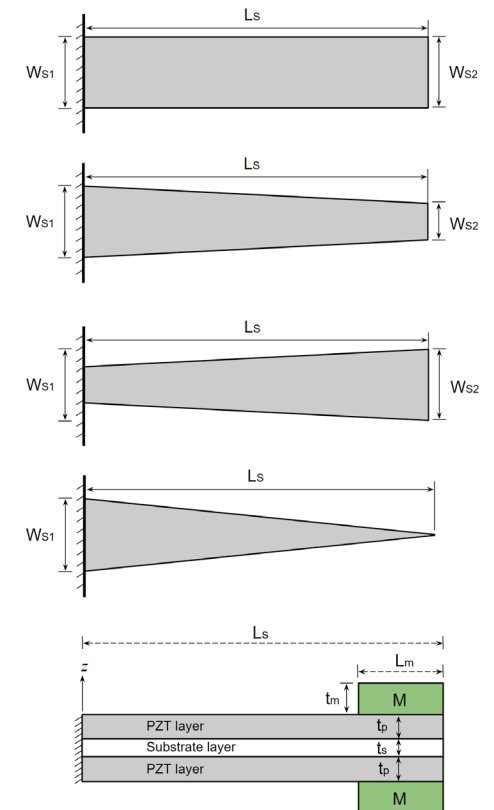
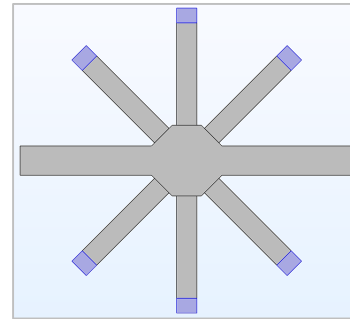


Fig. 2: A possible layout of the PEH system

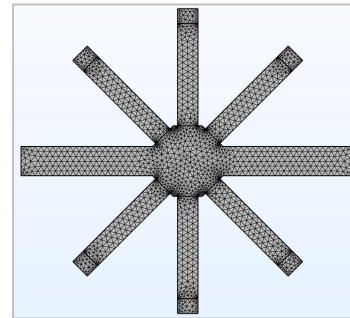


❖ CASE I: A multimodal PEH system

- ❑ Most of practical vibrations are **low frequencies that randomly change over time**, meaning that a multimodal EH could be much more efficient in harvesting vibration.
- ❑ The proposed layout is a multimodal system, in which **its first 4 modes are in a frequency range of 20 Hz** ($\cong 8, 12, 19, 27$ Hz, respectively).
- ❑ The output voltage levels are expected to be varied at different modal frequencies, since each resonance frequency has a unique mode shape, and generates a different level of stress on the surface of piezoelectric layers. However, compared to conventional layouts in which only the first resonance is excited by the ambient vibration, the output power generated by the proposed layout could be much higher in practice.

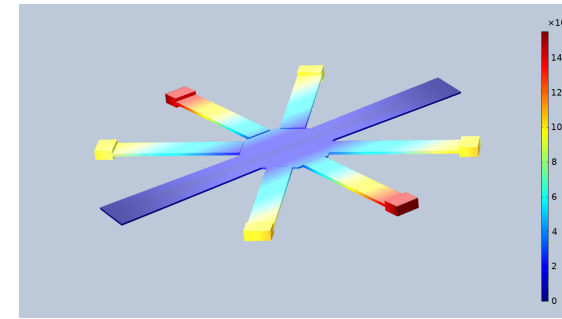


(Top view of the layout)

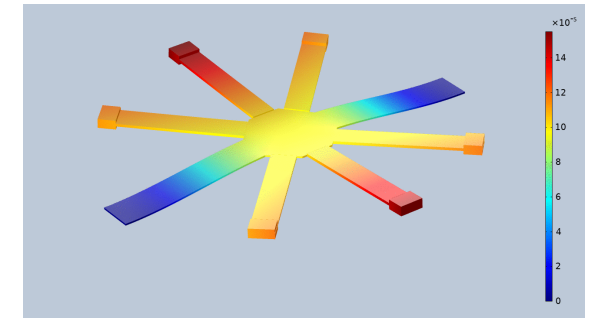


(Mesh)

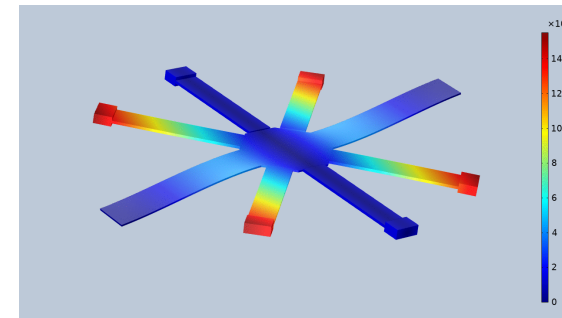
Results of Modal Analysis:



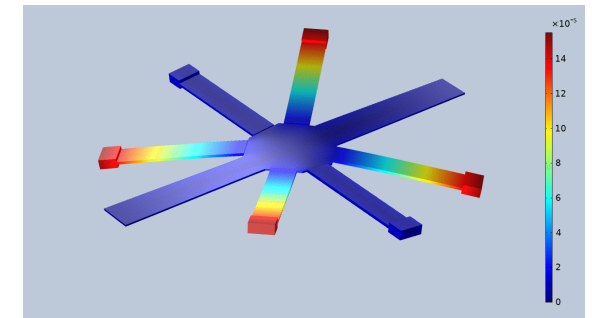
(Mode 1 – 8 Hz)



(Mode 2 – 12 Hz)



(Mode 3 – 19 Hz)

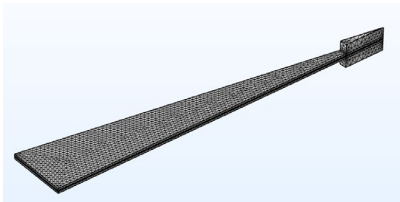
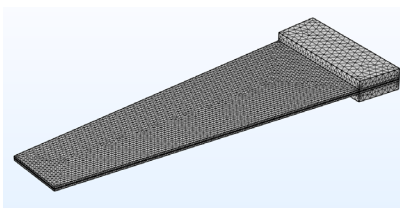
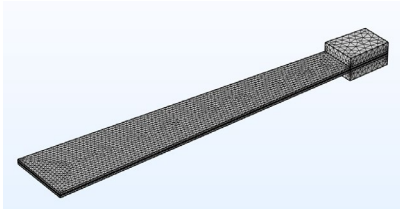
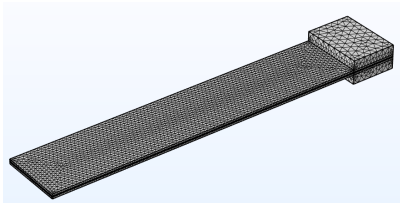


(Mode 4 – 27 Hz)

Primary beam ($45 \times 10 \times 0.5 \text{ mm}^3$), Secondary beams ($40 \times 7 \times 0.5 \text{ mm}^3$), Tip mass ($5 \times 7 \times 1 \text{ mm}^3$). Dimensions & Materials are provisional.

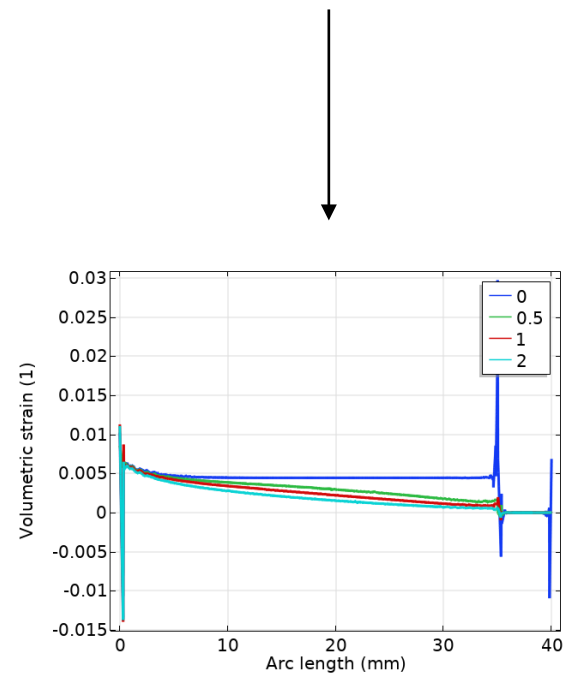
PZT-5H ($t = 0.2 \text{ mm}$), Aluminum substrate ($t = 0.1 \text{ mm}$), Primary beam is made of Polymethyl, Tip masses are made of Structural Steel

❖ CASE II: Shape-modified smart bimorph cantilevers



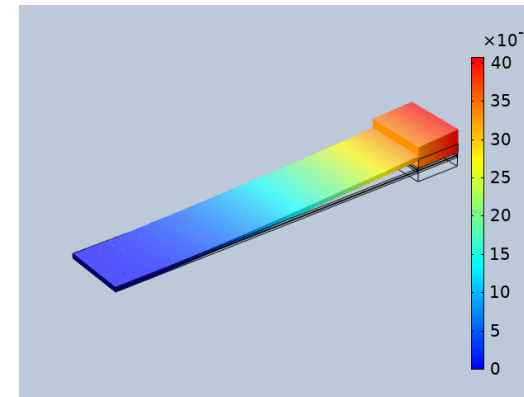
(Simulated smart cantilevers)

Results of Strain Analysis:

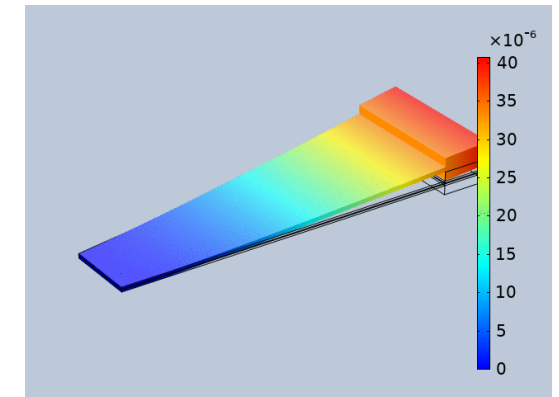


(Strain distribution in smart cantilever beams)

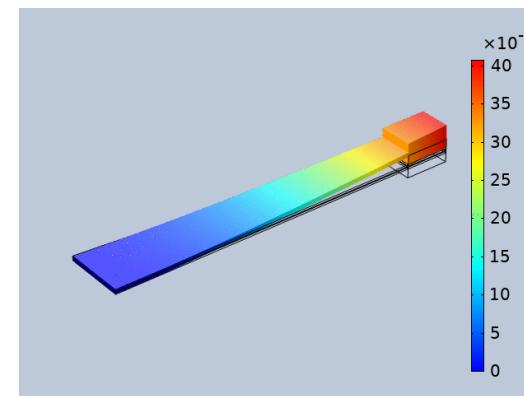
Results of Modal Analysis:



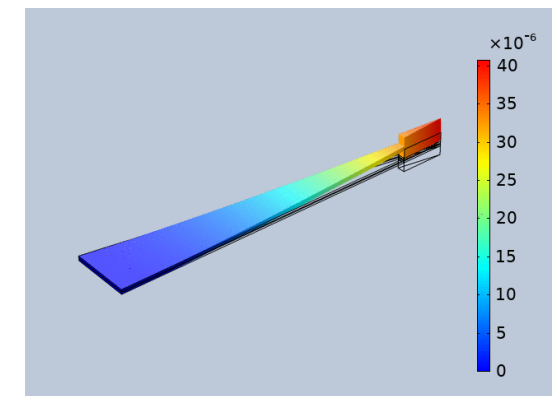
(Resonance: 93 Hz)



(Resonance: 74 Hz)



(Resonance: 118 Hz)



(Resonance: 255 Hz)

Electromechanical Modeling of Piezoelectric Smart Structures
Through Analytical Approaches

- As a case study, a **sandwich plate** made of FG substrate (e.g. made of **FGMs**, **porous** materials, ...) surrounded by piezoelectric layers is considered (Fig. 1).

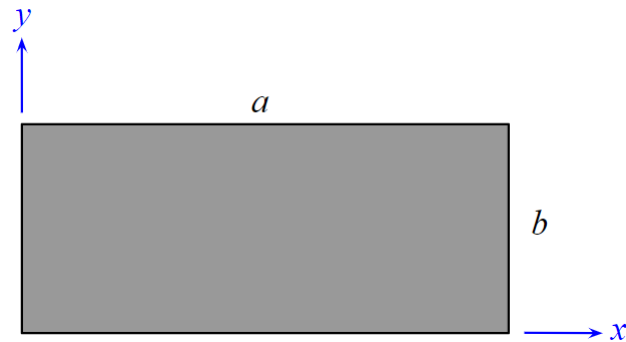


Fig. 1(a): Top view of the sandwich plate

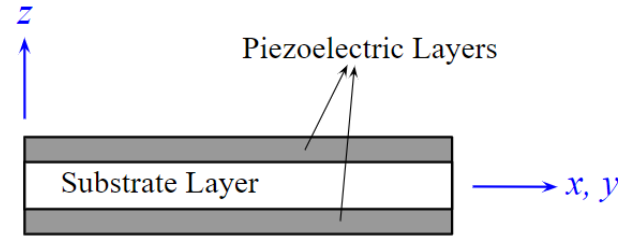


Fig. 1(b): Plate cross section

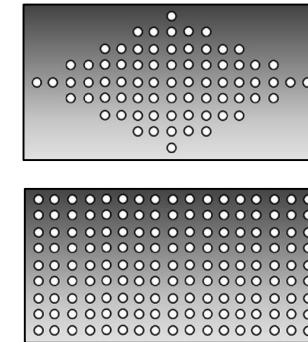


Fig. 1(c): FGMs containing porosity

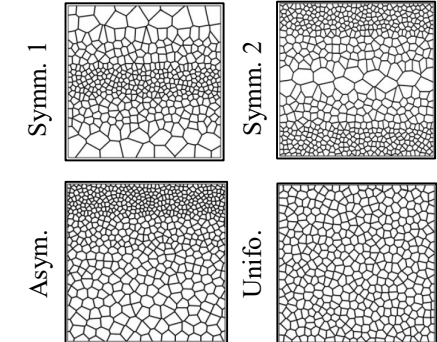


Fig. 1(d): Porous materials

- **Four-variable higher-order displacement models**, that include the effect of transverse shear deformations, is chosen to drive the equations of the system of interest (SOI).

Displacement Model

$$\begin{aligned}
 U_x(x, y, z) &= u_0(x, y) - z \frac{\partial w_b}{\partial x} - f(z) \frac{\partial w_s}{\partial x} \\
 U_y(x, y, z) &= v_0(x, y) - z \frac{\partial w_b}{\partial y} - f(z) \frac{\partial w_s}{\partial y} \\
 U_z(x, y, z) &= w_b(x, y) + w_s(x, y)
 \end{aligned}$$

- **Constitutive equations:**

- ❖ FGMs & porous free of fluid: $\{\sigma\} = [C]^s \{\varepsilon\}$
- ❖ Piezoelectrics: $\{\sigma\} = [C]^p \{\varepsilon\} - [e]^T \{E\}$, $\{D\} = [e] \{\varepsilon\} - [\Xi] \{E\}$
- ❖ Porous materials saturated by fluid: $\sigma_{ij} = 2G(z)\varepsilon_{ij} + \lambda_u \varepsilon_{kk} \delta_{ij} - \alpha(z)p\delta_{ij}$

► **Governing equations** derived from variational principle & Maxwell's Eq.:

$$\text{Eq. 1: } (a_{11})u_{0,xx} + a_{66}u_{0,yy} + (a_{12} + a_{66})v_{0,yx} + (-b_{12} - 2b_{66})w_{b,yyx} + (-b_{11})w_{b,xxx} + (-d_{12} - 2d_{66})w_{s,yyx} + (-d_{11})w_{s,xxx} = I_0\ddot{u}_0 - I_1\ddot{w}_{b,x} - J_1\ddot{w}_{s,x}$$

$$\text{Eq. 2: } (a_{66})v_{0,xx} + (a_{66} + a_{12})u_{0,yx} + (a_{11})v_{0,yy} + (-b_{11})w_{b,yyy} + (-2b_{66} - b_{12})w_{b,xyy} + (-d_{11})w_{s,yyy} + (-2d_{66} - d_{12})w_{s,xyy} = I_0\ddot{v}_0 - I_1\ddot{w}_{b,y} - J_1\ddot{w}_{s,y}$$

$$\begin{aligned} \text{Eq. 3: } & (b_{11})u_{0,xxx} + (b_{12} + 2b_{66})u_{0,yyx} + (b_{12} + 2b_{66})v_{0,yxx} + (b_{11})v_{0,yyy} + (-f_{11})w_{b,xxxx} + (-2f_{12} - 4f_{66})w_{b,yyxx} + (-f_{11})w_{b,yyy} + (-g_{11})w_{s,xxxx} \\ & + (-2g_{12} - 4g_{66})w_{s,yyxx} + r_1N_{cr}w_{b,xx} + r_2N_{cr}w_{b,yy} + r_1N_{cr}w_{s,xx} + r_2N_{cr}w_{s,yy} + (-g_{11})w_{s,yyy} + \hat{\mu}_1\phi_{0,xx} + \hat{\mu}_1\phi_{0,y} + q(x, y, z) \\ & = I_0(\ddot{w}_b + \ddot{w}_s) + I_1(\ddot{u}_{0,x} + \ddot{v}_{0,y}) - I_2(\ddot{w}_{b,xx} + \ddot{w}_{b,yy}) - J_2(\ddot{w}_{s,xx} + \ddot{w}_{s,yy}) \end{aligned}$$

$$\begin{aligned} \text{Eq. 4: } & (d_{11})u_{0,xxx} + (2d_{66} + d_{12})u_{0,xyy} + (d_{12} + 2d_{66})v_{0,yxx} + (d_{11})v_{0,yyy} + (-g_{11})w_{b,xxxx} + (-2g_{12} - 4g_{66})w_{b,yyxx} + (-g_{11})w_{b,yyy} \\ & + (-h_{11})w_{s,xxxx} + (-2h_{12} - 4h_{66})w_{s,yyxx} + (a_{55})w_{s,xx} + (-h_{11})w_{s,yyy} + (a_{55})w_{s,yy} + r_1N_{cr}w_{b,xx} + r_2N_{cr}w_{b,yy} + r_1N_{cr}w_{s,xx} + r_2N_{cr}w_{s,yy} \\ & + (\tilde{\mu}_1 + \mu_2)\phi_{0,xx} + (\tilde{\mu}_1 + \mu_2)\phi_{0,y} + q(x, y, z) = I_0(\ddot{w}_b + \ddot{w}_s) + J_1(\ddot{u}_{0,x} + \ddot{v}_{0,y}) - J_2(\ddot{w}_{b,xx} + \ddot{w}_{b,yy}) - K_2(\ddot{w}_{s,xx} + \ddot{w}_{s,yy}) \end{aligned}$$

$$\text{Eq. 5: } \lambda_7\nabla^2 w_s + \lambda_8\nabla^2 w_b + \lambda_9\phi_0 + \lambda_{10}\nabla^2\phi_0 + \lambda_{11}\nabla^2(u_{0,x} + v_{0,y}) + \lambda_{12}\nabla^4 w_b + \lambda_{13}\nabla^4 w_s = 0$$

► **Mechanical boundary conditions** derived from variational principle :

Essential BC's	Natural BC's	Essential BC's	Natural BC's
$\delta u_0 = 0$	$+n_x N_{xx} + n_y N_{xy} = 0$	$\delta w_b = 0$	$n_x(M_{xx,x}^b + M_{xy,y}^b) + n_y(M_{xy,x}^b + M_{yy,y}^b) + n_x N_{xx}^0(w_{b,x} + w_{s,x})$ $+ n_y N_{xy}^0(w_{b,x} + w_{s,x}) + n_x N_{xy}^0(w_{b,y} + w_{s,y})$ $+ n_y N_{yy}^0(w_{b,y} + w_{s,y}) = 0$
$\delta v_0 = 0$	$+n_x N_{xy} + n_y N_{yy} = 0$		
$\delta w_{b,x} = 0$	$-n_x M_{xx}^b - n_y M_{xy}^b = 0$	$\delta w_s = 0$	$n_x Q_{xz} + n_y Q_{yz} + n_x(M_{xx,x}^s + M_{xy,y}^s) + n_y(M_{xy,x}^s + M_{yy,y}^s)$ $+ n_x N_{xx}^0(w_{b,x} + w_{s,x}) + n_y N_{xy}^0(w_{b,x} + w_{s,x})$ $+ n_x N_{xy}^0(w_{b,y} + w_{s,y}) + n_y N_{yy}^0(w_{b,y} + w_{s,y}) = 0$
$\delta w_{b,y} = 0$	$-n_x M_{xy}^b - n_y M_{yy}^b = 0$		
$\delta w_{s,x} = 0$	$-n_x M_{xx}^s - n_y M_{xy}^s = 0$		
$\delta w_{s,y} = 0$	$-n_x M_{xy}^s - n_y M_{yy}^s = 0$		

► Solution approaches:

Galerkin Approach
(General BC's)

$$u_0(x, y) = \sum_{m=1}^{\infty} \sum_{n=1}^{\infty} A_{mn} F'_m(x) F'_n(y) e^{i\omega t}$$

$$v_0(x, y) = \sum_{m=1}^{\infty} \sum_{n=1}^{\infty} B_{mn} F_m(x) F'_n(y) e^{i\omega t}$$

$$w_b(x, y) = \sum_{m=1}^{\infty} \sum_{n=1}^{\infty} C_{mn} F_m(x) F_n(y) e^{i\omega t}$$

$$w_s(x, y) = \sum_{m=1}^{\infty} \sum_{n=1}^{\infty} D_{mn} F_m(x) F_n(y) e^{i\omega t}$$

$$\phi_0(x, y) = \sum_{m=1}^{\infty} \sum_{n=1}^{\infty} E_{mn} F_m(x) F_n(y) e^{i\omega t}$$

$$[B]\{\bar{X}_{mn}\} = 0$$

$$|B| = 0$$

↓
Frequencies, Buckling loads, ...

State Space Approach
(Levy-type BC's)

$$u_0(x, y) = \sum_{m=1}^{\infty} U_{0m}(x) \sin(\eta_m y) e^{i\omega t}$$

$$v_0(x, y) = \sum_{m=1}^{\infty} V_{0m}(x) \cos(\eta_m y) e^{i\omega t}$$

$$w_b(x, y) = \sum_{m=1}^{\infty} W_{bm}(x) \sin(\eta_m y) e^{i\omega t}$$

$$w_s(x, y) = \sum_{m=1}^{\infty} W_{sm}(x) \sin(\eta_m y) e^{i\omega t}$$

$$\phi_0(x, y) = \sum_{m=1}^{\infty} \phi_{0m}(x) \sin(\eta_m y) e^{i\omega t}$$

$$\{Z'\} = [T]\{Z\}$$

$$\{Z\} = e^{Tx}\{K\}$$

$$e^{Tx} = [V][e^{\lambda x}][V]^{-1}$$

↓
[B]\{Z\} = 0 → [H]\{K\} = 0 → |H| = 0 → Results

Decoupling Approach
(Levy-type BC's)

We introduce ϕ_1 and ϕ_2 as

$$\phi_1 = u_{0,x} + v_{0,y}$$

$$\phi_2 = u_{0,y} - v_{0,x}$$

↓
5 coupled PDE's will be reduced to 2 independent ODE's, which can be simply solved.

$$[B]\{\bar{X}_{mn}\} = 0$$

$$|B| = 0$$

↓
Frequencies, Buckling loads, ...

Navier Approach
Simply-supported BC's

$$u_0(x, y) = \sum_{m=1}^{\infty} U_{0m} \cos(\eta_m x) \sin(\eta_n y) e^{i\omega t}$$

$$v_0(x, y) = \sum_{m=1}^{\infty} V_{0m} \sin(\eta_m x) \cos(\eta_n y) e^{i\omega t}$$

$$w_b(x, y) = \sum_{m=1}^{\infty} W_{bm} \sin(\eta_m x) \sin(\eta_n y) e^{i\omega t}$$

$$w_s(x, y) = \sum_{m=1}^{\infty} W_{sm} \sin(\eta_m x) \sin(\eta_n y) e^{i\omega t}$$

$$\phi_0(x, y) = \sum_{m=1}^{\infty} \phi_{0m} \sin(\eta_m x) \sin(\eta_n y) e^{i\omega t}$$

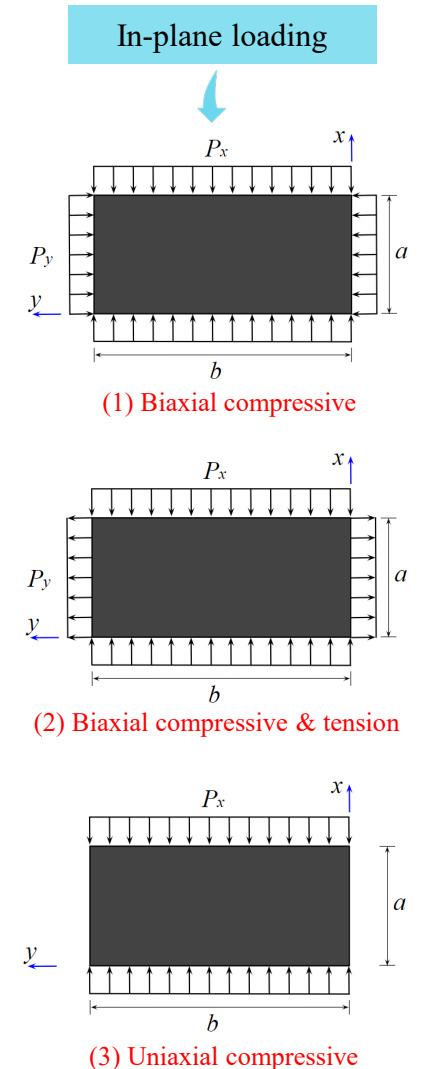
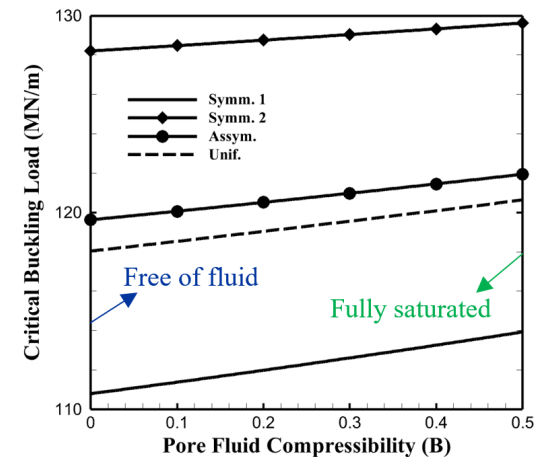
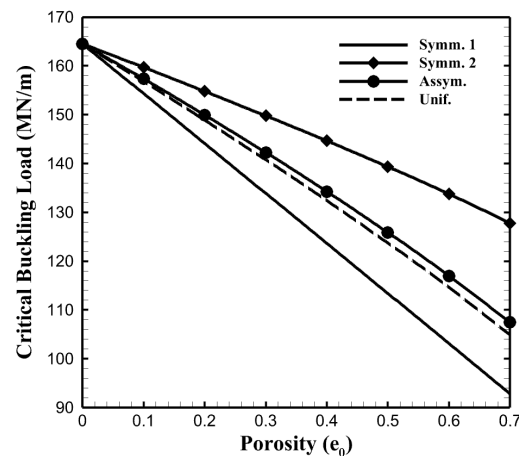
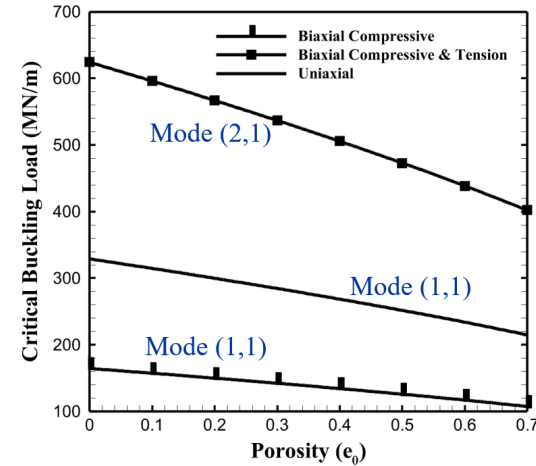
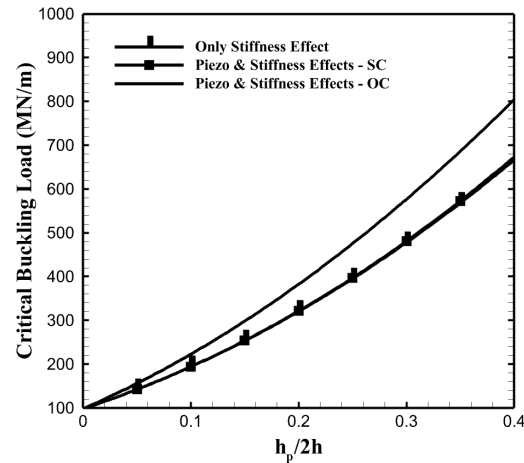
$$[B]\{\bar{X}_{mn}\} = 0$$

$$|B| = 0$$

↓
Frequencies, Buckling loads, ...

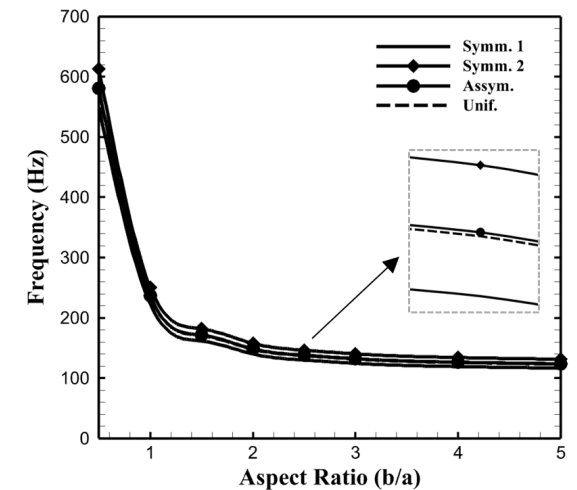
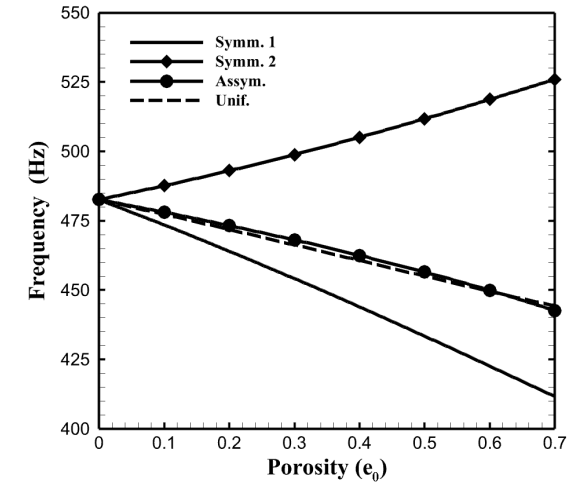
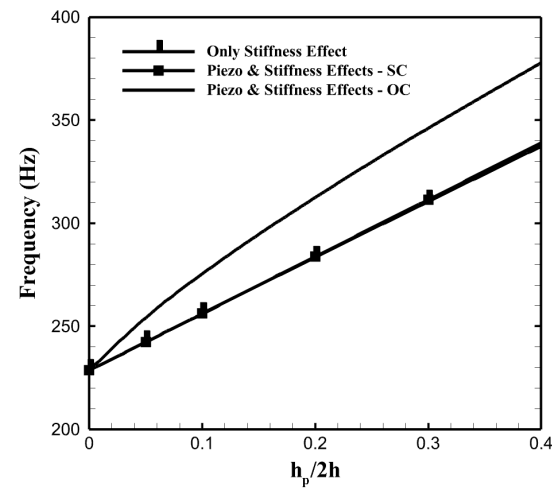
- Preliminary results of **Buckling** analysis of piezoelectric bimorph plates with porous core:

- Electrical effect of piezoelectric layers, and porosity coefficient play significant roles in buckling response.
- Values of critical buckling load are highly dependent on the **type of porosity distribution**.
- In some cases, buckling phenomenon occurs in **higher buckling modes**.



► Preliminary results of **Free Vibration** of piezoelectric bimorph plates with porous core:

- **Electrical effect of piezoelectric layers, and porosity coefficient** play significant roles in vibration characteristics of smart porous plates.
- Variation of natural frequency due to changes in porosity is highly dependent on the **type of porosity distribution**.
- Different frequency responses were observed for various Electrical and mechanical boundary conditions.



► Preliminary results of **Wave Propagation analysis** of piezoelectric bimorph plates with porous core:

Using the harmonic method, the displacement field for the wave propagation is defined as:

$$u_0(x, y) = U_{0m} e^{i(k_1 x + k_2 y - \omega t)}$$

$$v_0(x, y) = V_{0m} e^{i(k_1 x + k_2 y - \omega t)}$$

$$w_b(x, y) = W_{bm} e^{i(k_1 x + k_2 y - \omega t)}$$

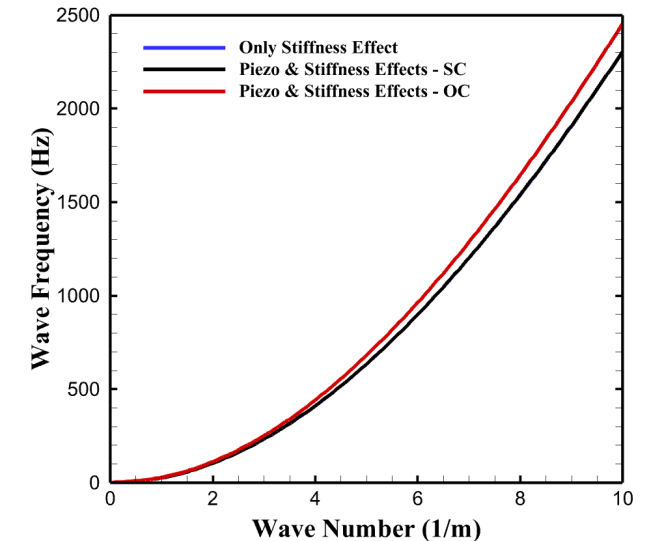
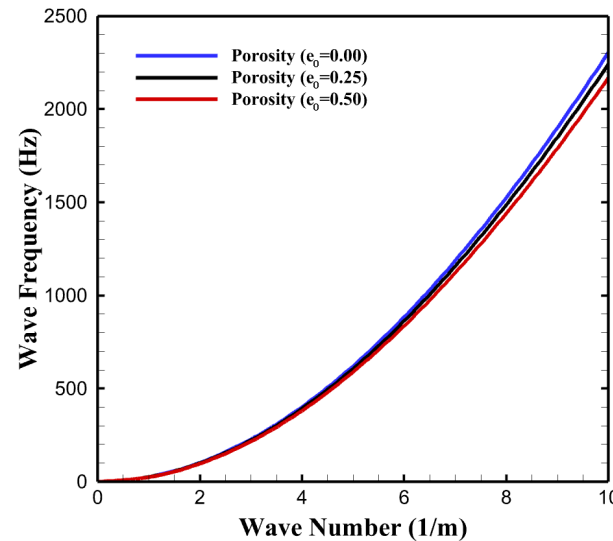
$$w_s(x, y) = W_{sm} e^{i(k_1 x + k_2 y - \omega t)}$$

$$\phi_0(x, y) = \phi_{0m} e^{i(k_1 x + k_2 y - \omega t)}$$

k_1 and k_2 are wave numbers in x and y directions, respectively, and ω indicate the circular frequency. Substituting the above expressions in governing equations results in:

$$([K] - \omega^2 [M])\{U_i\} = 0$$

- As was observed in buckling and vibration analyses, Electrical effect of piezoelectric layers plays an important role in propagation of wave in smart porous piezoelectric plates. Material characteristics were also found to have significant effect on wave propagation features.





actuators



Article

Electromechanical Vibration Characteristics of Porous Bimorph and Unimorph Doubly Curved Panels

Mahmoud Askari ^(*), Eugenio Brusa and Cristiana Delprete

Department of Mechanical and Aerospace Engineering, Politecnico di Torino, Corso Duca degli Abruzzi 24, 10129 Torino, Italy; eugenio.brusa@polito.it (E.B.); cristiana.delprete@polito.it (C.D.)

* Correspondence: mahmoud.askari@polito.it

Received: 6 January 2020; Accepted: 23 January 2020; Published: 28 January 2020



JSA

Original Article

On the vibration analysis of coupled transverse and shear piezoelectric functionally graded porous beams with higher-order theories

Mahmoud Askari ^(*), Eugenio Brusa and Cristiana Delprete

J Strain Analysis
1–21
© IMechE 2020
Article reuse guidelines:
sagepub.com/journals-permissions
DOI: 10.1177/0309324720922085
journals.sagepub.com/home/sdj
SAGE

Recent Topics on Mechanics and Materials in Design

PAPER REF: 120

VIBRATION ANALYSIS OF POROUS BIMORPH DOUBLY CURVED SHELLS FOR ENERGY HARVESTING APPLICATIONS

Mahmoud Askari^(*), Eugenio Brusa¹, Cristiana Delprete¹¹Department of Mechanical and Aerospace Engineering (DIMEAS), Politecnico di Torino, Italy^(*)Email: mahmoud.askari@polito.it

Thank You for Your Attention!

Q & A?